Proton transfer in functionalized phosphonic acid molecules

ARTICLE *in* PHYSICAL CHEMISTRY CHEMICAL PHYSICS · JANUARY 2010

Impact Factor: 4.49 · DOI: 10.1039/b917903h · Source: PubMed

2 AUTHORS:

Chen Wang
Centers for Disease Control and Prevention
13 PUBLICATIONS **73** CITATIONS
SEE PROFILE

Stephen J Paddison
University of Tennessee
128 PUBLICATIONS **3,950** CITATIONS
SEE PROFILE

Proton transfer in functionalized phosphonic acid molecules

Chen Wang and Stephen J. Paddison*

Received 2nd September 2009, Accepted 5th November 2009
First published as an Advance Article on the web 30th November 2009
DOI: 10.1039/b917903h

Ionomers with protogenic groups such as phosphonic acid have recently been proposed as suitable polymer electrolyte membranes for fuel cells operating with little humidification due to their extraordinary amphotericity. The hydrogen bonding and energetics associated with proton transfer of substituted phosphonic acid molecules and their self-condensation products (anhydride + H_2O) are examined through *ab initio* electronic structure calculations. The global minimum energy structures of methyl-, phenyl-, benzyl-, trifluoromethyl- and phenyldifluoro-phosphonic acids determined at the B3LYP/6-311G** level indicate that the fluorinated molecules exhibit slightly stronger binding to water than the non-fluorinated molecules. The potential energy profiles for transfer of a proton within the condensation products were obtained at the B3LYP/6-311G** level for each of the acids, and revealed that the trifluoromethyl system has the lowest endothermicity (5.3 kcal mol^{-1}) in contrast to the methyl system which has the greatest endothermicity (7.1 kcal mol^{-1}) and a barrier of 7.6 kcal mol^{-1}. When no constraints are imposed on the system, proton transfer from the anhydride to a water molecule (primary) is accompanied by a secondary proton transfer (from protonated water molecule back to the anhydride) in all cases except the trifluoromethyl anhydride where charge separation and formation of a hydronium ion occurs. It appears that the secondary proton transfer would substantially determine the emergence of transition states and the correlated endothermicities.

1. Introduction

Fuel cells have gained tremendous interest in the past two decades as highly efficient devices for converting chemical energy into electrical energy. Due to the many promising characteristics as a power source, proton exchange membrane (PEM) fuel cells are widely considered the most applicable energy conversion system for use in automobiles and portable devices.[1] Efficient operation of the PEM fuel cell depends on the rate of transport of protons through the electrolyte (*i.e.* from anode to cathode), thus requiring a separator material with high proton conductivity (*i.e.* >0.1 S cm^{-1}) under a range of operating conditions. In another words, not only does the electrolyte perform as a separator in anode and cathode, it is also fundamentally relevant for the operational efficiency of the device.[2]

Perfluorosulfonic acid (PFSA) membranes are the most commonly used fuel cell electrolytes with Nafion®, originally developed by DuPont in the 1960s, the benchmark ionomer. PFSA membranes consist of a highly hydrophobic polytetrafluoroethylene (PTFE) backbone with pendant perfluoroether side chains terminating with highly hydrophilic sulfonic acid groups. The hydrophilic domains are formed when the material is exposed to water through the aggregation of the sulfonic acid groups, and the dissociated protons deriving from the solvation of acidic groups become mobile, facilitating the transport of protons. The presence of water is a crucial factor in forming charge carriers and enabling the transport of protons.[3–6] Proton transport in this two-phase system is due to both structural diffusion[7–10] (*i.e.* proton hopping) and vehicular diffusion.[2,11,12] Nafion exhibits high proton conductivity (approximately 0.19 S cm^{-1}) only when fully hydrated (*i.e.* 100% relative humidity).[13] The demand for high humidification of PFSA membranes limits the maximum operating temperature to 100 °C if the pressure is restrained to approximately 1 atm. Thus, modification of Nafion-type polymers[14–16] were developed for operation at temperatures up to nearly 130 °C to prevent the rapid loss of conductivity associated with decreasing humidity. Another serious problem is the "cross-over" of water due to electroosmotic drag, which consequently leads to complicated heat and water management schemes. Moreover, impurity in hydrogen derived from reformate tends to poisoning (*i.e.* CO adsorption) of platinum based catalysts at operating temperatures less than 120 °C.[12,17] A simple approach to weaken the adsorption of CO on catalyst particles is to increase the temperature, thus enhancing the CO tolerance of the fuel cell.[18] Hence, it is essential to find alternative membrane materials which retain both the high proton conductivity and the chemical stability in the absence of water.

Recently, efforts have been undertaken to explore proton-conducting ionomers in which the conduction is independent of the presence of an aqueous phase. Simply replacing the water with another appropriate proton solvent, which features the same ability to transport protons at higher temperatures, is regarded as a fundamental approach in achieving this goal.[19] Several polymer blends with phosphoric acid (or sulfuric acid)[20]

Department of Chemical & Biomolecular Engineering, University of Tennessee, Knoxville, TN 37996, USA. E-mail: spaddison@utk.edu

have been investigated in recent years, where the acid acts as a substitute for water. Another feasible approach is to construct fully polymeric systems in which the proton conductivity largely relies on the intrinsic properties of the system. Kreuer *et al.*[21] have proposed several nitrogen-containing aromatic heterocycles as proton conductors, including imidazole, pyrazole and benzimidazole. These materials show moderate proton conductivity at high temperatures (*i.e.* >100 °C)[21] due to their amphotericity and self-dissociation which are similar to water. Attempts to improve conductivity were achieved by means of adding extrinsic charger carriers such as an acidic polymer[12] or improving the intermolecular proton transport.[19,22] High proton conductivity (*i.e.* $\leq 7 \times 10^{-4}$ S cm^{-1} at 200 °C) with such a solvent was obtained in a fully polymeric system by Herz and co-workers,[23] where flexible spacers or segments were introduced to connect the heterocycles with polystyrene or polysiloxane architectures. This connection somewhat suppresses the long-range diffusion of the proton solvent but gives a certain local mobility, which promotes the intrinsic conduction within heterocycles due to breaking and forming of dynamic hydrogen bonds.[19] Despite possessing similar properties as water, the heterocycles have a fundamental drawback which is their relatively low self-dissociation. This weakness leads to only moderate conductivity and hence, the discovery of other protogenic groups capable of functioning as both a proton solvent and proton source may be a key to addressing this limitation.

Phosphonic acid (PA) exhibits potentially significant advantages for use in fuel cell electrolytes when compared to sulfonic acid and imidazole.[24,25] The conductivity of neat PA is relatively high,[26–28] due to the nature of the hydrogen bonding and amphoteric characteristics. The high strength of the carbon–phosphorus bond increases the thermal stability of the compound for operation at high temperatures. The experimental results from Schuster *et al.*[25] show that phosphonic acid molecules have a high conductivity under conditions of low humidity and intermediate temperature. A recent study of this high proton conductivity[26] reveals that the structural diffusion is still the dominant mechanism whereas a certain degree of vehicular diffusion arises due to the slightly "weaker" hydrogen bonding than in phosphoric acid. Examination of the instability related to electrochemical reaction and thermal-oxidation[25] suggests that PA based polymers maintain a better stability in a wide range of temperature while imidazole based ones are severely vulnerable to oxidation at high temperatures. A recent computational study has provided insight into the differences of alkyl PA molecules.[29] These calculations revealed that the water binding is stronger and the energy penalty for proton transfer lower in alkyl phosphonic acid molecules than in either imidazole or sulfonic acid functionalized alkanes. The latter is in agreement with the observed higher proton conductivity in the $-PO_3H_2$ molecules.[25] Quantum mechanical calculations have been undertaken in an investigation of the mechanisms of proton transfer (*i.e.* proton hopping) in neat phosphoric acid,[30,31] liquid PA,[32] and heptyl PA.[33]

Diverse phosphonic acid functional polymers have received significant interest as intrinsically conducting membrane materials, including perfluorovinylethers,[34,35] polytrifluorostyrenes,[36,37] polyphenylsulfones,[38,39] polyphosphazenes,[40,41] and other grafted copolymers.[34] Several synthetic approaches have also been implemented to assess various PAs.[27,28] Furthermore, alkyl,[25,29] aryl[42] and perfluoroalkyl[27] groups linked to the PA and the backbone have been suggested as a means of improving the properties of the materials.

Here we focus on quantifying the underlying effects of different chemical groups adjacent to a PA moiety through electronic structure calculations. Specifically, the effects of five different groups located on the α-site of a mono PA are evaluated, including methyl, phenyl, benzyl, trifluoromethyl, and phenyldifluoromethyl. The hydrogen bonding and binding of a single water molecule are compared amongst these substituted PAs, and the hydrogen bond interactions within paired PA dimers are assessed. The energetics for the transfer of a proton are computed in the constitutional isomer of the acid dimers (*i.e.* the PA anhydride + H_2O) due to the experimental observation of self-condensation products in PA functionalized polymers with ^{31}P NMR.[43–45] The latter study indicated that the self-condensation becomes more pronounced at low water contents and higher temperature and hence in our present work we have pursued systems with no added water. Finally, energy profiles associated with the transfer of a proton in each of the systems are computed and compared.

Our manuscript is organized as follows: the first section contains a short description of the computational methods used to determine structure and energetics for all molecular systems. This methods section is followed by a discussion section describing the structures and binding energies with each of the PA molecules with a single water molecule, the PA dimers, and the PA anhydrides. The discussion then covers the energetics of the proton transfer in each of PA anhydrides. Concluding remarks follow the discussion section.

2. Computational methods

All molecular orbital calculations were performed with the Gaussian 03 suite of programs.[46] Fully optimized geometries of phosphonic acid molecules, using conjugate gradient methods[47] without symmetry constraints, were computed initially using Hartree–Fock theory with the 6-31G** split valence basis set.[48–50] Further refinement of the structures was obtained by employing hybrid density functional theory (DFT) with Becke's 3 parameter functional (B3LYP)[51,52] with the same basis set and then with the larger 6-311G** set.[53] Minimum energy structures of each acid with a single water molecule were determined at the B3LYP/6-311G** level. Subsequently, vibrational frequencies and zero point energies (ZPEs) for both the PAs and PA + H_2O acids were calculated employing the same level of theory. Molecular binding energies of water molecules and acid monomers were determined from both the uncorrected and ZPE corrected total electronic energies. The counterpoise (CP) method of Boys and Bernardi[54,55] was employed to compute the effect of basis set superposition error (BSSE)[56–58] on all the computed binding energies. It is well known that DFT does not always correctly

describe the interaction of neutral molecules particularly the hydrogen bonding of aromatic molecules.[59] Hence, insight into the strength of the interaction of these molecules from the computed binding energies is only in a relative comparison amongst the different PAs. Starting from the fully optimized structure, minimum energy conformations (B3LYP/6-311G**) were obtained for each of the PA dimers and anhydrides employing the same scheme. For the anhydride system, various geometrically constrained conditions were implemented to assess their effects on proton transfer. In an initial set of calculations, the distance between the oxygen atom of the anhydride donating the proton and the oxygen atom of the water molecule receiving the proton was fixed along with the length of the OH bond unpaired with the water molecule. Only the positions of the two oxygen atoms involved in the transfer of the proton were fixed in a second set of calculations. No constraints were imposed during the transfer of the proton in the final set of calculations. Potential energy surface (PES) scans at the B3LYP/6-311G** level were performed to obtain profiles of the energy associated with the proton transfer under each of the conditions described above. These scans are based on optimized static structures and as such only reveal the relative tendencies in the proton transfer energetics, not absolute values. A transition state (TS) structure was obtained for each of the principal proton transfers with a TS optimization and subsequent verification by the calculation of a single imaginary frequency.

3. Results and discussion

3.1 $R–PO_3H_2 + H_2O$

Fully optimized structures of five different PA molecules were determined and the minimum energy structures at the B3LYP/6-311G** level of theory for methyl (Me), phenyl (Ph), benzyl (Bn), trifluoromethyl (CF_3), and phenyldifluoromethyl ($PhCF_2$) substituted phosphonic acids, each hydrogen bonded to a single water molecule, are displayed in Fig. 1(a)–(e), respectively. The O···O distance for the hydrogen bond between a water molecule and each of the PA molecules along with the corresponding O–H bond length for an acidic proton of the acid, the latter in parentheses, is indicated in each of the figures. The total electronic energies of all structures both uncorrected and corrected for ZPE, along with binding energies inclusive of ZPE and BSSE for each of the acids with a water molecule are presented in Table 1.

These equilibrium structures indicate that a water molecule adopts a similar orientation with each of the PA molecules with both a donating and accepting hydrogen bond. The position of the water molecule is essentially identical in the methyl and benzyl phosphonic acids and very slightly closer (as measured by the accepting hydrogen bond) with the phenyl phosphonic acid. The O–H bond length of the acidic proton is slightly longer than observed in an isolated methyl phosphonic acid molecule (0.96 Å).[29] The binding energies (last three columns of Table 1) of the water molecule to these three acids are all quite similar with the phenyl substituted acid about

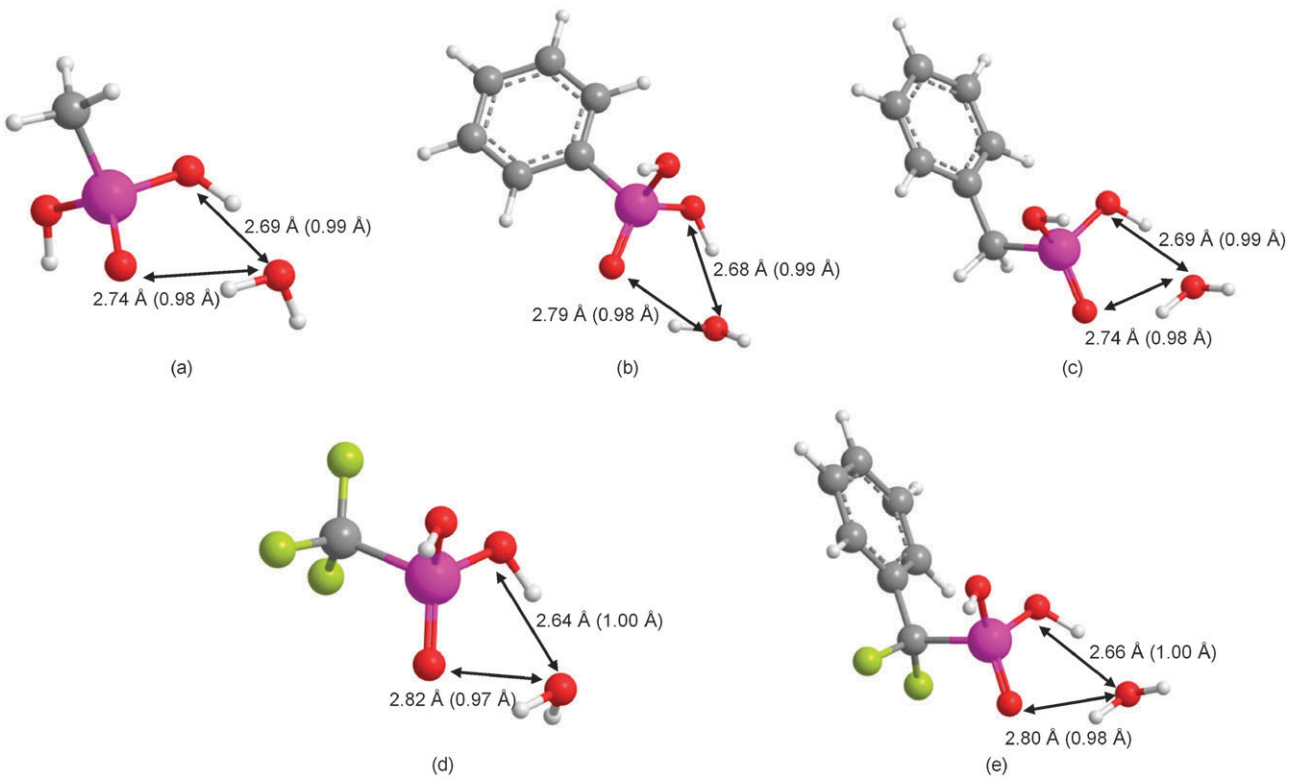

Fig. 1 Fully optimized (B3LYP/6-311G**) global minimum energy structures of phosphonic acid with a single water molecule (a) MePA + H_2O; (b) PhPA + H_2O; (c) BnPA + H_2O; (d) $CF_3PA + H_2O$; (e) $PhCF_2PA + H_2O$. The distances of two hydrogen bonds are presented and the lengths of O–H bonds are listed in the parentheses. The BSSE corrected binding energy of water molecule in the above systems is: −9.4, −8.9, −9.6, −10.1 and −9.8 kcal mol^{-1}, respectively.

Table 1 Energies for phosphonic acids[a]

	E_{elec}[b]	E_{elec} + ZPE[c]	ΔE^d/kcal mol^{-1}	ΔE_{ZPE}[e]/kcal mol^{-1}	ΔE_{BSSE}[f]/kcal mol^{-1}
Me-PA	−608.3321600	−608.260910			
Ph-PA	−800.1066031	−799.981739			
Bn-PA	−839.4334625	−839.280768			
CF_3-PA	−906.1156495	−906.068018			
$PhCF_2$-PA	−1037.9517487	−1037.815817			
Me-PA + H_2O	−684.8058899	−684.708634	−16.5	−13.5	−9.4
Ph-PA + H_2O	−876.5793462	−876.428888	−15.9	−13.2	−8.9
Bn-PA + H_2O	−915.9073248	−915.728822	−16.6	−13.8	−9.6
CF_3-PA + H_2O	−982.5905494	−982.516725	−17.2	−14.2	−10.1
$PhCF_2$-PA + H_2O	−1114.4259265	−1114.263920	−16.8	−13.8	−9.8

[a] For structures optimized at the B3LYP/6-311G** level. [b] Total electronic energy in Hartrees. [c] Total electronic energy corrected for zero point energy (ZPE) in Hartrees. [d] Binding energy based on (uncorrected) total electronic energies. [e] Binding energy based on ZPE corrected E_{elec}. [f] Binding energy based on CP correction to BSSE for structures optimized under CP scheme with ZPE correction.

0.5 kcal mol^{-1} weaker when corrections for ZPE and BSSE are implemented. The H_2O molecule adopts a position considerably closer in the CF_3- and the $PhCF_2$-PAs and the acidic H^+ resides somewhat closer ($\approx$0.06 Å) to the oxygen atom with the length of the O–H bond about 1 Å. The former is quite similar to that observed for trifluoromethane sulfonic acid (CF_3SO_3H) where at the B3LYP/6-31G** level the O···O distance and O–H bond length were computed to be 2.60 and 1.02 Å, respectively.[60,61] The presence of the strong electron withdrawing group in the α-position to the oxoacid enhances the proton dissociation and appears to slightly increase the binding of the water molecule to the acid.

3.2 Phosphonic acid dimers

The structure and energetics were determined for dimers of each PA (PADs). The simplest case is a dimer composed of a pair of PA monomers sharing double hydrogen bonds. The possible *trans* and *cis* conformations were examined by comparing their relative electronic energies and binding energies and these are reported in Table 2. The fully optimized structures of only the lowest energy conformation for each of the different PAs, calculated at the B3LYP/6-311G** level, are shown in Fig. 2.

Prior work indicated that the methyl phosphonic acid dimer (MePAD) exhibits two identical hydrogen bonds (as indicated by the O···O distances) and corresponding O–H bond distances in each dimer and in each conformation.[29] The calculated energies also revealed that the *trans* and *cis* MePAD are nearly isoenergetic. However, it is not clear whether the substitution of a methyl group tends to alter the geometry or energetics of the dimer. Thus, PADs with diverse substituents were examined using a similar scheme.

The most favourable conformation (*trans* or *cis*) of each PAD was identified from the energies listed in Table 2. The PhPAD exhibits a *trans* conformation (see Fig. 2a) with the two benzene rings well separated rather than the *cis* conformation to avoid steric hindrance with the aromatic rings. As a result, the (ZPE corrected) total energy of the *trans* conformation is approximately 0.34 kcal mol^{-1} lower than that of the *cis* conformation. However, slightly distorted *cis* conformations (see Fig. 2b and d) are more energetically favourable for the BnPAD and $PhCF_2$PAD where the aromatic ring is not directly bonded to the phosphorus atom. It was also determined that the *cis* conformations are 0.13 and 0.19 kcal mol^{-1} (corrected for ZPE) lower than the corresponding *trans* conformations for the BnPAD and $PhCF_2$PADs, respectively. Similar to the case of MePAD,[29] only a 0.09 kcal mol^{-1} energy difference (corrected for ZPE) was observed between the *trans* and *cis* CF_3PAD (Fig. 2c) suggesting that there is no particular conformational preference.

The analysis of the hydrogen bonding is insightful for understanding the interactions between the acid pairs. The minimum energy structures of the PADs (shown in Fig. 2) reveal that both the O···O and O–H bond distances involved in the hydrogen bonds are largely unaffected by the presence of the different substituents. Specifically, the O–H bond lengths in the hydrogen bonds are essentially the

Table 2 Energetics of phosphonic acid dimers[a]

	E_{elec}[b]	E_{elec} + ZPE[c]	ΔE^d/kcal mol^{-1}	ΔE_{ZPE}[e]/kcal mol^{-1}	ΔE_{BSSE}[f]/kcal mol^{-1}
Ph-PA dimer (*cis*)	−1600.2530573	−1600.001683	−25.0	−24.0	−20.3
Ph-PA dimer (*trans*)	−1600.2537273	−1600.002233	−25.4	−24.3	−20.4
CF_3-PA dimer (*cis*)	−1812.2723470	−1812.174320	−25.8	−24.0	−20.1
CF_3-PA dimer (*trans*)	−1812.2722224	−1812.174001	−25.7	−23.8	−20.0
Bn-PA dimer (*cis*)	−1678.9088206	−1678.601649	−26.3	−25.2	−21.3
Bn-PA dimer (*trans*)	−1678.9085618	−1678.601440	−26.1	−25.0	−21.3
$PhCF_2$-PA dimer (*cis*)	−2075.9457932	−2075.671447	−26.5	−25.0	−21.0
$PhCF_2$-PA dimer (*trans*)	−2075.9456974	−2075.671288	−26.5	−24.9	−21.0

[a] For structures optimized at the B3LYP/6-311G** level. [b] Total electronic energy in Hartrees. [c] Total electronic energy corrected for zero point energy (ZPE) in Hartrees. [d] Binding energy based on (uncorrected) total electronic energies. [e] Binding energy based on ZPE corrected E_{elec}. [f] Binding energy based on CP correction to BSSE for structures optimized under CP scheme with ZPE correction.

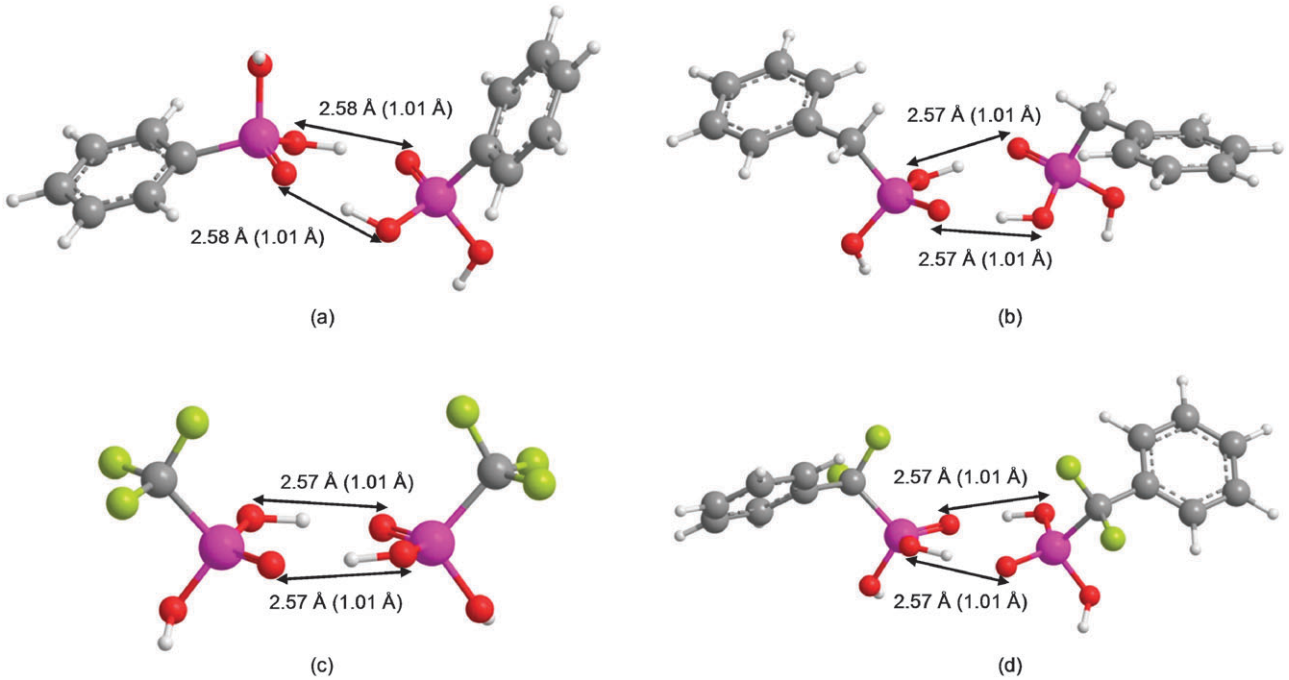

Fig. 2 Fully optimized (B3LYP/6-311G**) global minimum energy structures of: (a) *trans*-phenyl; (b) *cis*-benzyl; (c) *cis*-trifluoromethyl; and (d) *cis*-phenyldifluoromethyl phosphonic acid dimers. The distances of two hydrogen bonds are presented and the lengths of O–H bonds are listed in parentheses. The hydrogen bonds in these acid pairs are approximately the same as are the BSSE corrected binding energy of these pairs.

same (1.01 Å) and slightly longer than those not involved in hydrogen bonding (0.96 Å). This geometric similarity is consistent with the associated binding energy listed in Table 2.

3.3 Phosphonic acid anhydrides

The mechanism of proton transfer in phosphonic acid based polymers is complex due to the coexistent condensation reaction of phosphonic acids, producing phosphonic acid anhydride (PAA) and water:

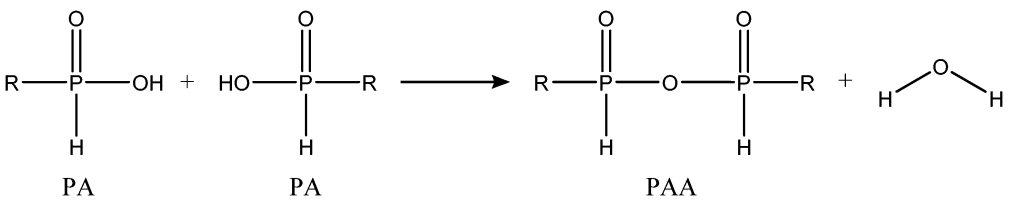

Theoretical and experimental studies[30,44] have suggested that the self-condensation reactions in phosphoric and phosphonic acids may reduce proton mobility through interruption of proton hopping pathways formed by the hydrogen bonding of the acids. If water escapes from the system the proton conductivity typically falls substantially. Investigations[43,44] on the self-condensation of poly-vinyl-phosphonic acid (PVPA) show that a certain extent of condensation leads to a considerable amount of PAA product (about 30%) and free water under nearly dry conditions at high temperatures ($\leq$150 °C). Therefore, the coexistence of water with the anhydrides should be considered in order to understand the mechanism of proton transport in neat phosphonic acid and in polymeric systems involving PA. As a consequence, the geometries and energies associated with proton transfer of the anhydrides functionalized with the various chemical groups were compared.

Fully optimized structures of the PAAs with the various substituents were obtained using the protocol described earlier. Dissimilar to the situations in the monomers, the intramolecular hydrogen bonding provides increased stability for the anhydride. This interaction may also account for the fact that all PAAs tend to be more stable as *cis*-conformations while *trans*-conformations seem to be affected by the steric strain from the side groups.

Complexes consisting of a single water molecule and an anhydride were optimized at the B3LYP/6-311G** level. These global minimum energy structures are shown in Fig. 3, where the distances of the hydrogen bonds between the anhydrides and water molecules are indicated and the corresponding O–H bond lengths given in parentheses. With the introduction of fluorine atoms, the acidity of the PAAs appears to increase as indicated by the shorter hydrogen bonds in the fluorinated molecules. It is not surprising that the shortest O···O distance (2.55 Å) was observed in the trifluoromethyl system which is nearly 0.04 Å shorter than the

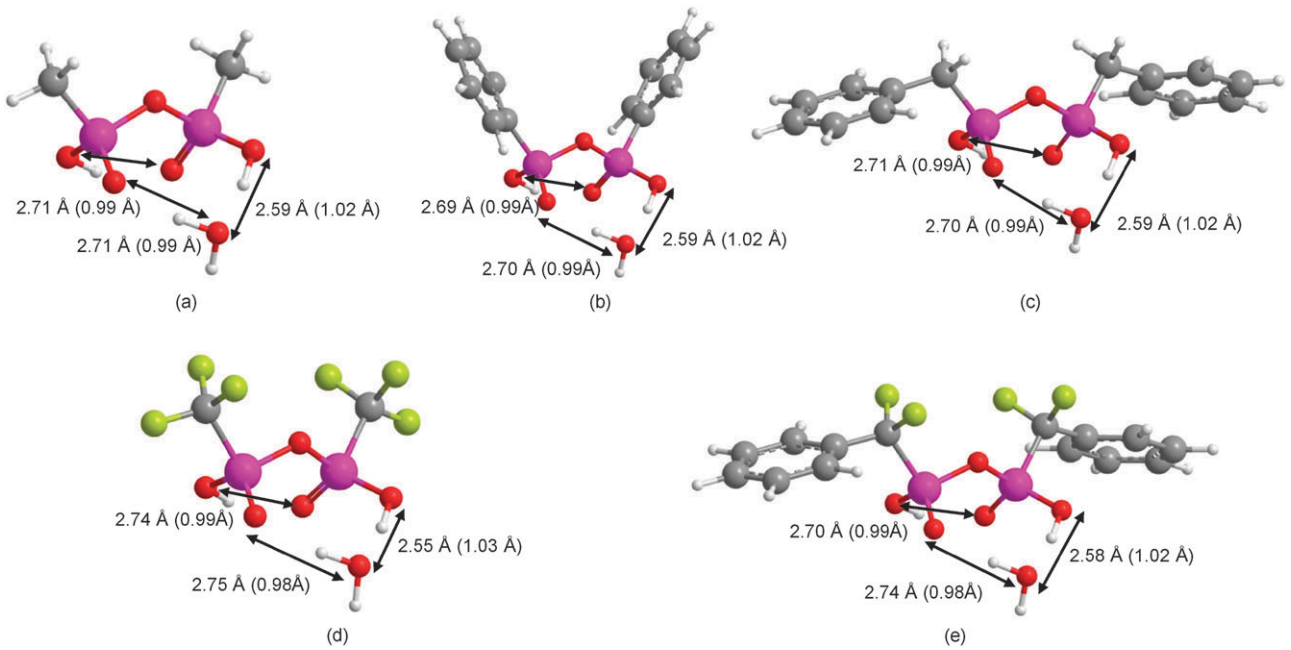

Fig. 3 Fully optimized (B3LYP/6-311G**) global minimum energy structures of: (a) methyl; (b) phenyl; (c) benzyl; (d) trifluoromethyl; and (e) phenyldifluoromethyl phosphonic acid anhydrides each with a single water molecule. The distances of the three hydrogen bonds in each system are given and the O–H bond lengths shown in the parentheses. The BSSE corrected binding energy of the water molecule in the above systems is: −13.9, −13.7, −14.1, −16.7 and −15.8 kcal mol^{-1}, respectively.

nonfluorinated molecules. The shorter hydrogen bonds typically facilitate easier proton transfer if charge separation is possible.[29]

The energetics of the phosphonic acid anhydrides and the PAAs each with a single water molecule are reported in Table 3. Binding energies computed from the ZPE and BSSE corrected electronic energies at the B3LYP/6-311G** level provide evidence that the fluorinated groups bind water more tightly than the other groups. The trifluoromethyl system has a binding energy of −16.7 kcal mol^{-1}, which is nearly 3 kcal mol^{-1} greater than any of the non-fluorinated molecules and 2.7 kcal mol^{-1} more than the difluorinated molecules. We have computed the difference in the energy of the phosphonic acid dimer and its isoelectronic PAD + H_2O and report them in the sixth column of Table 3. It is clear that in all cases the ZPE corrected energy of the gas phase PADs are lower than the energies of their corresponding condensation products, particularly for the fluorinated molecules where $(CF_3PO_3H_2)_2$ is 9.5 kcal mol^{-1} lower in energy than CF_3HO_2P–O–PO_2HCF_3 + H_2O. This result is in contrast to the observed condensation products in real PA systems (as discussed above) and hence in an effort to assess the effects that a medium might have on the formation of water in phosphonic acid based electrolytes we optimized both the PADs and the PAD + H_2O systems in a continuum dielectric solvent (ε = 78.4) using the Onsager model[62] as implemented in G03.[63–65] It is important to note, however, that the dielectric constant of PEMs even under conditions of high relative humidity is much lower than that of bulk water.[66–69] Furthermore, the PA based electrolytes of interest in this study are those that are nominally dry or of minimal hydration. Comparison of the energy differences of

Table 3 Energetics of phosphonic acid anhydrides[a]

	E_{elec}[b]	E_{elec} + ZPE[c]	ΔE_{ZPE}[d]/kcal mol^{-1}	ΔE_{BSSE}[e]/ kcal mol^{-1}	E_{PAA}–E_{PAD}[f]/ kcal mol^{-1}	$(E_{PAA}$–$E_{PAD})_s$[g]/ kcal mol^{-1}
Me-PAA	−1140.2179666	−1140.097071				
Ph-PAA	−1523.7672537	−1523.539460				
Bn-PAA	−1602.4210993	−1602.137533				
CF_3-PAA	−1735.7722142	−1735.698418				
Ph CF_2-PAA	−1999.4514518	−1999.201059				
Me-PAA + H_2O	−1216.7003241	−1216.553821	−19.2	−13.9	4.4	2.2
Ph-PAA + H_2O	−1600.2486153	−1599.995644	−18.9	−13.7	3.8	2.3
Bn-PAA + H_2O	−1678.9036317	−1678.594567	−19.4	−14.1	4.4	2.8
CF_3-PAA + H_2O	−1812.2582817	−1812.158915	−21.6	−16.7	9.5	9.3
Ph CF_2-PAA + H_2O	−2075.9361587	−2075.660285	−20.8	−15.8	6.9	6.0

[a] For structures optimized at the B3LYP/6-311G** level. [b] Total electronic energy in Hartrees. [c] Total electronic energy corrected for zero point energy (ZPE) in Hartrees. [d] Binding energy based on ZPE corrected E_{elec}. [e] Binding energy based on CP correction to BSSE for structures optimized under CP scheme with ZPE correction. [f] Difference in ZPE corrected energy of PAA + H_2O and PA dimer. [g] Difference in energy of PAA + H_2O and PA dimer in dielectric solvent (ε = 78.4) with the Onsager model.

the dimers and their associated monohydrated anhydrides in the dielectric solvent (final column of Table 3) with those obtained in the gas phase clearly show an increase in the relative stability of the PAA + H_2O systems. Interestingly, this increased propensity to form the condensation products in the dielectric solvent is not uniform amongst the different functionalized phosphonic acids with the largest (and by far most significant) differences observed for the alkyl (*i.e.*, CH_3– and $C_6H_5CH_2$–) molecules. Only minor changes in the electronic energies where observed in the fluorinated molecules with the dimers remaining significantly more stable than their corresponding anhydrides.

3.4 Proton transfer in monohydrated phosphonic acid anhydrides

There are three possible 'pathways' where proton transfer may occur due to the intramolecular hydrogen bonds within these systems. Two of the proton transfers may occur between the acid anhydride and the water molecule: either the acid acts as the proton donor and the water molecule acts as a proton acceptor, or the water molecule acts as a proton donor that facilitates proton transfer to the acid. In the third case, an intramolecular transfer within the acid anhydride is also possible. We are primarily interested in the proton transfer from acid anhydride to water, and for the sake of clarity this is referred to as the 'principal transfer'. The three O···O distances indicated in each of the systems in Fig. 3 clearly show that the hydrogen bond over which this proton transfer occurs is significantly shorter than the other two hydrogen bonds. Hence, these other possible proton transfers are referred to as secondary transfers. Various constraints were applied in each molecular system to understand factors affecting the principal transfer from acid to water. Both the oxygen–oxygen separation distance in the principal transfer and the length of the O–H bond in the acid–acid hydrogen bond were constrained in the first case. Only the O···O distance (over which the proton transfer occurs) was fixed in the second case and no restriction placed on the O–H bond, allowing for an intramolecular or 'back transfer' of a proton. In the third case no constraints were imposed on any bond lengths or interatomic distances.

Potential energy surface scans were performed under each of these three cases at the B3LYP/6-311G** level. The relative energy profiles for proton transfer in the methyl, phenyl, benzyl, trifluoromethyl, and phenyldifluoromethyl substituted systems for the first and third cases (described above) and are shown in Fig. 4–8, respectively. We have plotted all of the energy profiles as a function of the asymmetric stretching coordinate, q_{asym}, ($q_{asym} = \frac{1}{\sqrt{2}}(r_{O1\cdots H} - r_{H\cdots O2})$) to facilitate comparison to proton transfer energetics obtained for other systems included the Zundel ion in bulk water.[70–72] The O···O and O–H bond distances of the three hydrogen bonds without restrictions were examined at each step of the scan to provide insight into the correlation between the principal and secondary proton transfers. It is clear from these energy profiles that intrinsic proton transfer will occur between the phosphonic acids due to the inherent amphotericity, but there is an energy penalty associated with this process.

The O···O distances are shown for each of the PAAs at the completion of the PES under the relaxed case (3rd case described above) in the configuration on the right side in each of the Fig. 4–8. When both constraints were removed (third case described above) the barrier for the proton transfer shifts quite substantially (nearly 0.1 Å) towards the products. This is probably due to the contraction of the O···O distance during the proton transfer, but upon transfer to the anhydride this O···O distance increases to a length very similar to that observed in the reactant molecule (see Fig. 3). When compared to the corresponding fully optimized structures in Fig. 3 it is clear that the intramolecular hydrogen bond (shown at the back of each figure) is shortened for all PAAs but particularly so for the methyl-, phenyl-, and benzyl-substituted molecules

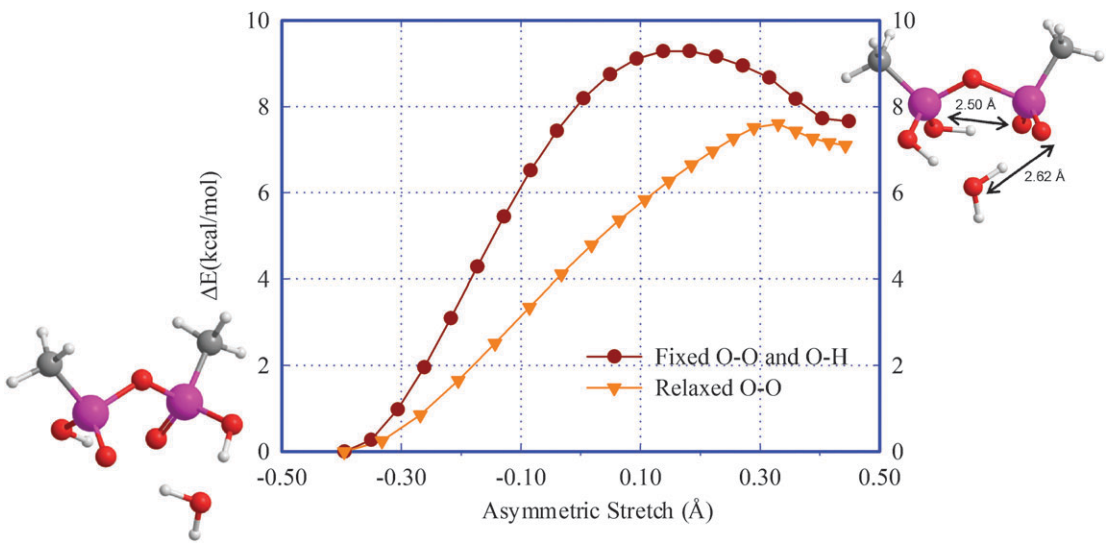

Fig. 4 Relative energy profiles (at the B3LYP/6-311G** level) for transferring a proton from methyl phosphonic acid anhydride to a water molecule as a function of the asymmetric stretch coordinate. The potential energy curves were obtained from scans performed under 2 different conditions: (1) fixed O···O and O–H distances; and (2) relaxed O···O distance. The height of the energy barrier under the constrained conditions is about 9.2 kcal mol^{-1}, while that for the unconstrained case is 7.6 kcal mol^{-1}.

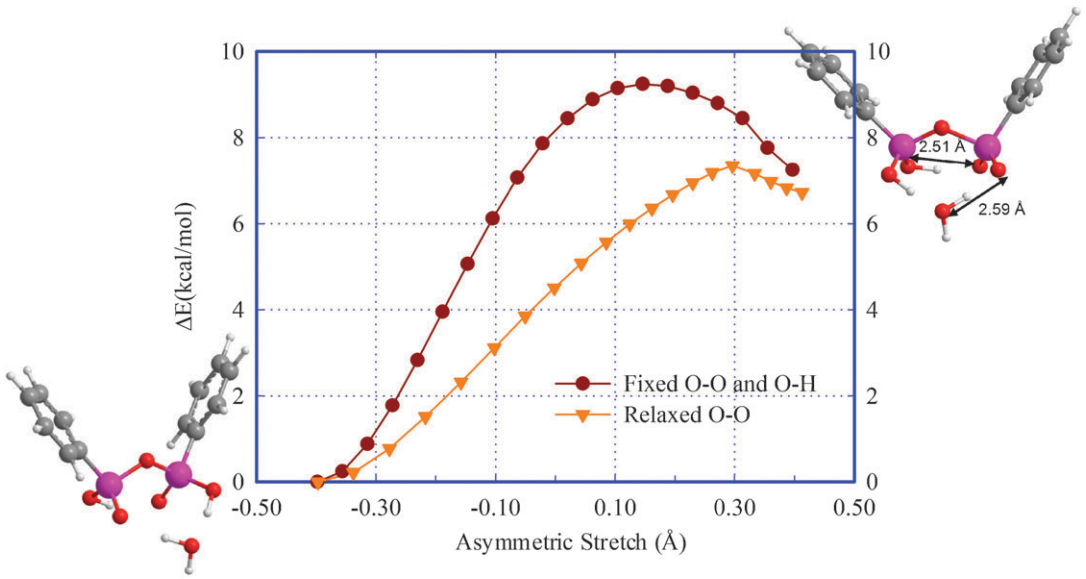

Fig. 5 Relative energy profiles (at the B3LYP/6-311G** level) for transferring a proton from phenyl phosphonic acid anhydride to a water molecule as a function of the asymmetric stretch coordinate. The potential energy curves were obtained from scans performed under 2 different conditions: (1) fixed O···O and O–H distances; and (2) relaxed O···O distance. The height of the energy barrier under the constrained conditions is about 9.2 kcal mol^{-1}, while that for the unconstrained case is 7.3 kcal mol^{-1}.

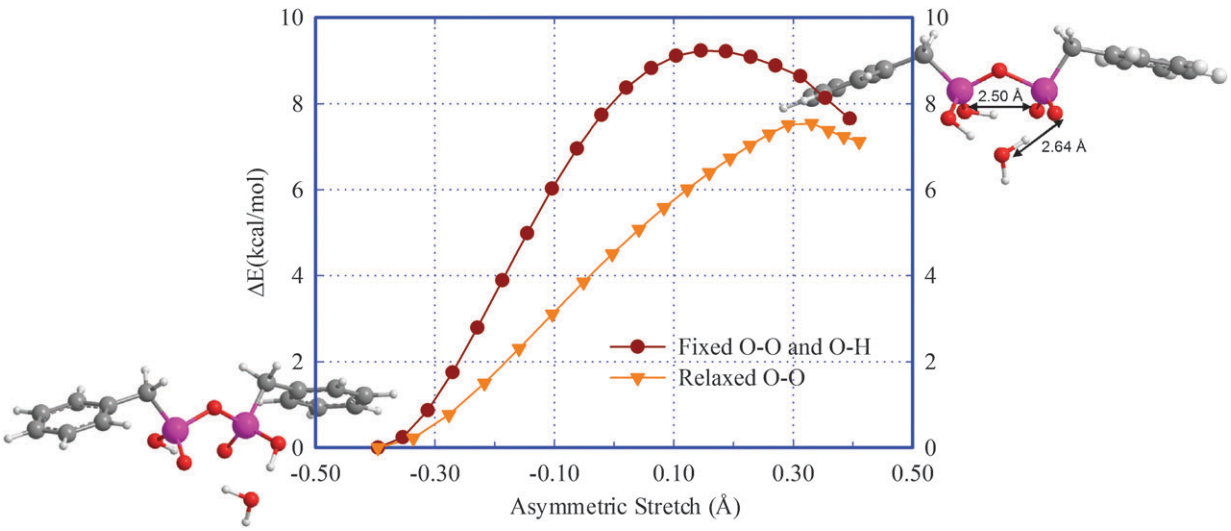

Fig. 6 Relative energy profiles (at the B3LYP/6-311G** level) for transferring a proton from benzyl phosphonic acid anhydride to a water molecule as a function of the asymmetric stretch coordinate. The potential energy curves were obtained from scans performed under 2 different conditions: (1) fixed O···O and O–H distances; and (2) relaxed O···O distance. The height of the energy barrier under the constrained conditions is about 9.2 kcal mol^{-1}, while that for the unconstrained case is 7.5 kcal mol^{-1}.

where typically the contraction is about 0.2 Å. However, in no case did intramolecular proton transfer accompany the principal transfer.

The pertinent O···H bond distances for the 3 protons involved in the three hydrogen bonds of the five PAA + H_2O systems were plotted as a function of the asymmetric stretch coordinate in an effort to determine whether the principal and secondary proton transfers are correlated. The profiles are shown for the CH_3- and CF_3-PAAs in Fig. 9 and 10, respectively, as these display the extremes in the results obtained for the various anhydrides. Common to all PAAs is the observation that no intramolecular proton transfer occurs as the O5–H bond is only very slightly lengthened during the entire principal proton transfer. However, the two systems display qualitatively different behaviour in the secondary proton transfer where in the Me-PAA the proton on the water molecule is 'back' transferred to the PAA in a stepwise fashion, but in CF_3-PAA no secondary proton transfer occurs and only a slight increase in the O2–H bond occurs during the completion of the principal proton transfer. Evidently the much acidity of the fluorinated anhydride seems to prohibit the proton transfer from the water molecule to occur.

The endothermicity and energy barriers were calculated from the relative potential energies and are reported in

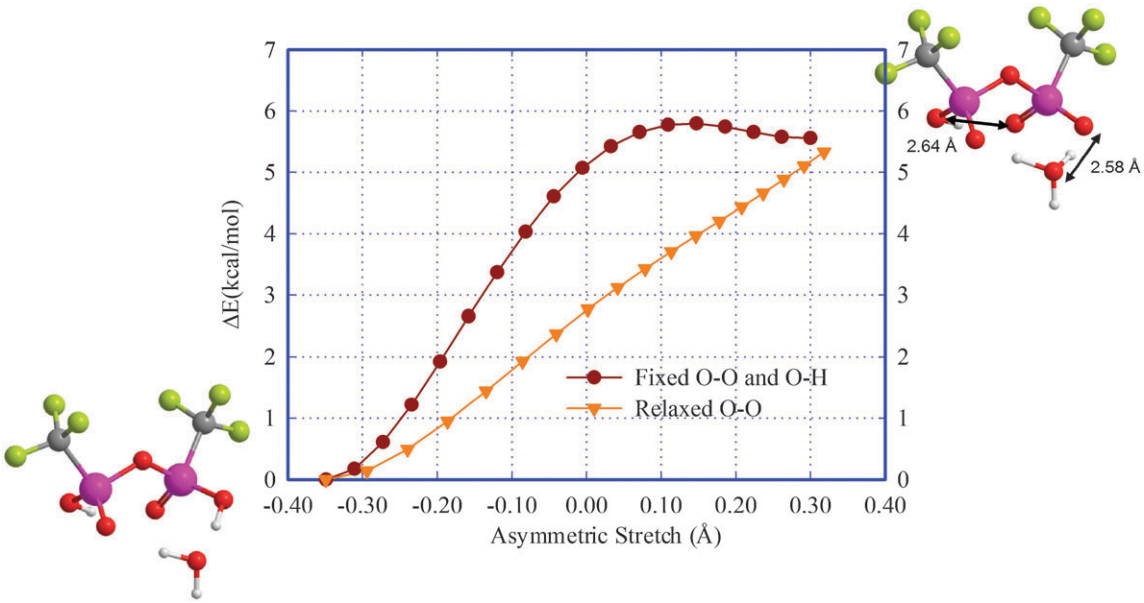

Fig. 7 Relative energy profiles (at the B3LYP/6-311G** level) for transferring a proton from trifluoro-methyl phosphonic acid anhydride to a water molecule as a function of the asymmetric stretch coordinate. The potential energy curves were obtained from scans performed under 2 different conditions: (1) fixed O···O and O–H distances; and (2) relaxed O···O distance. The height of the energy barrier under the constrained conditions is about 5.8 kcal mol^{-1}. No energy barrier associated with the proton transfer was obtained when no constraints were imposed.

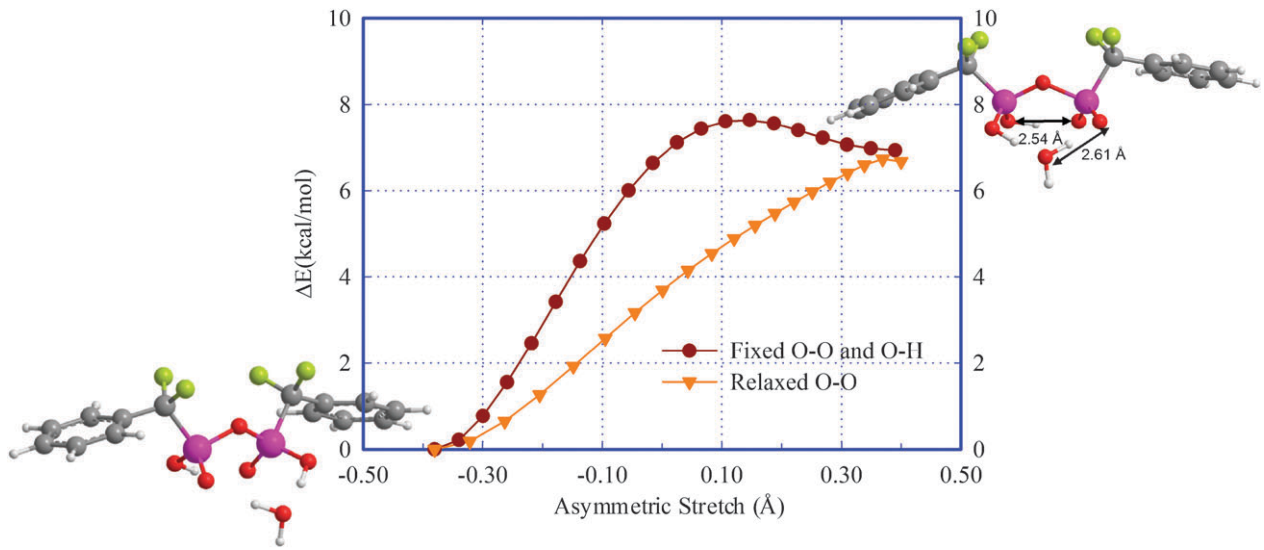

Fig. 8 Relative energy profiles (at the B3LYP/6-311G** level) for transferring a proton from phenyl-difluoromethyl phosphonic acid anhydride to a water molecule as a function of the asymmetric stretch coordinate. The potential energy curves were obtained from scans performed under 2 different conditions: (1) fixed O···O and O–H distances; and (2) relaxed O···O distance. The height of the energy barrier under the constrained conditions is about 7.6 kcal mol^{-1}, while that for the unconstrained case is 6.7 kcal mol^{-1}.

Table 4. Consistent with previous work,[29] the non-fluorinated PAAs show the greatest barrier to the proton transfer with all barriers greater than 7 kcal mol^{-1} under conditions without any constraints and more than 9 kcal mol^{-1} when constraints are imposed. The CF_3-substituted PAA gave the lowest endothermicity when all atoms were relaxed of only slightly more than 5.3 kcal mol^{-1}, and interestingly was the only system where no barrier (*i.e.*, no transition state) accompanied the proton transfer. Undoubtedly, this later finding is related to the observation that there is no secondary transfer (from the protonated water back to the anhydride) in the CF_3-PAA, as seen with all the other PAAs. The principal proton transfer results in charge separation and the formation of the contact ion pair: $CF_3HO_2P–O–P(CF_3)O_2^-·H_3O^+$. Charge separation is critical to long range proton transfer[73] and hence one may conclude that the fluorinated PA polymers may exhibit the highest proton conductivities. Transition states for each of the PAAs were determined (with the method described above) for proton transfer performed without any imposed constraints with the exception of $(CF_3HO_2P)_2O$. The effects on these

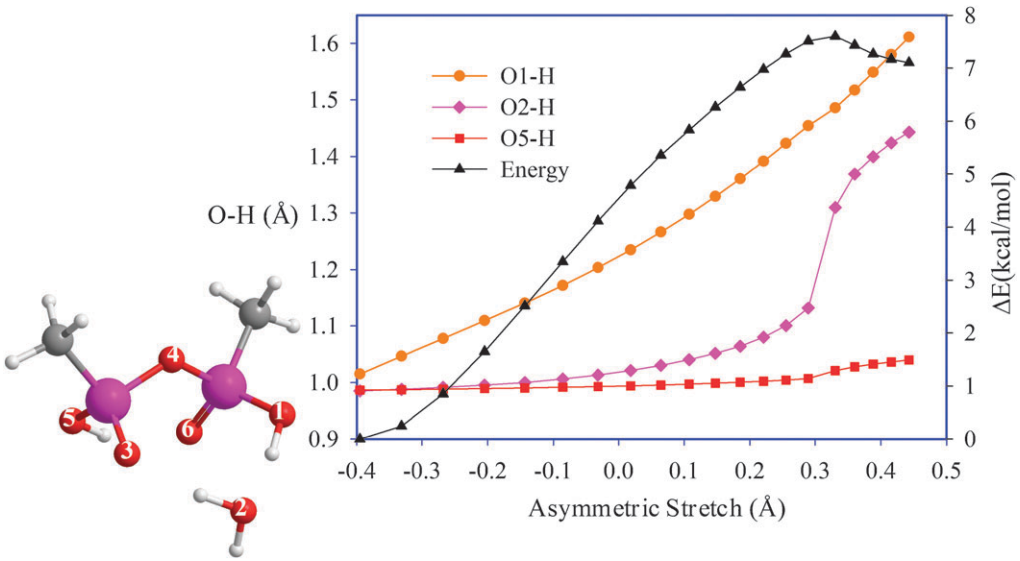

Fig. 9 The O–H bond distances in the methyl phosphonic acid anhydride + H_2O system as a function of the asymmetric stretch coordinate during the potential energy scan of the 'principal' proton (from O1 to O2) transfer determined at the B3LYP/6-311G** level. The plots clearly reveal the essentially stepwise nature of proton transfer where with the back transfer of a proton from the water molecule occurs towards the completion of the proton transfer from the anhydride and is accompanied with a slight decrease in the energy.

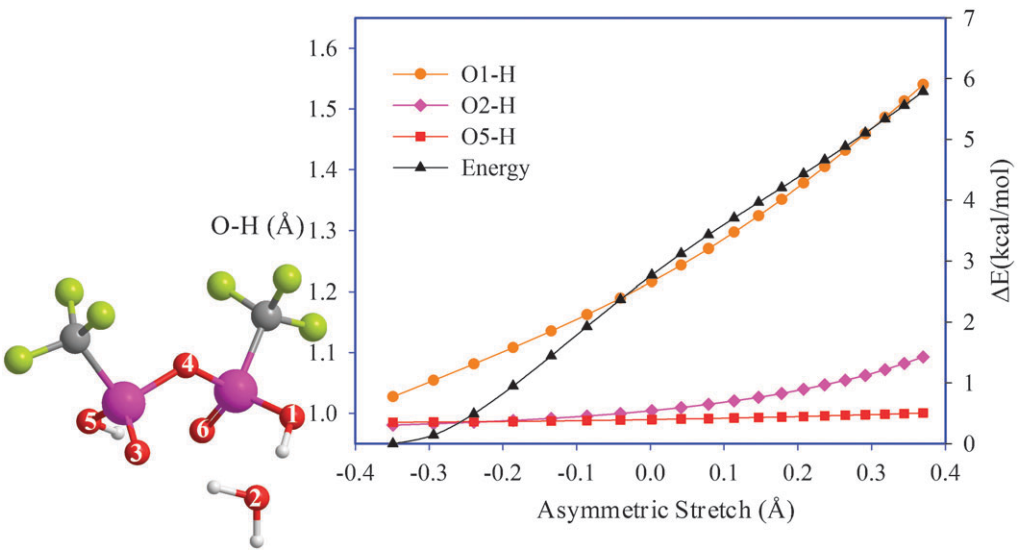

Fig. 10 The O–H bond distances in the trifluoromethyl phosphonic acid anhydride + H_2O system as a function of the asymmetric stretch coordinate during the potential energy scan of the 'principal' proton (from O1 to O2) transfer determined at the B3LYP/6-311G** level. The plots reveal that no secondary (neither intramolecular nor back transfer from the H_2O) proton transfer occurs.

Table 4 Proton transfer energetics for PAAs[a,b]

	Fixed O···O[c]		Fixed O···O and O–H[c]		Relaxed[c]		Solvated[d]	
	TB[e]	E[f]	TB[e]	E[f]	TB[e]	E[f]	TB[e]	E[f]
Me-PAA + H_2O	9.23	7.36	9.29	7.66	7.60	7.10	5.42	5.26
Ph-PAA + H_2O	9.24	6.66	9.29	7.07	7.34	6.65	5.35	5.25
Bn-PAA + H_2O	9.18	7.07	9.23	7.47	7.54	7.04	5.76	5.35
CF_3-PAA + H_2O	5.77	5.49	5.79	5.56	—[g]	5.33	—[g]	1.15
Ph CF_2-PAA + H_2O	7.60	6.88	7.63	6.97	6.80	6.73	5.25	5.12

[a] Structures optimized at the B3LYP/6-311G** level. [b] All entries in kcal mol^{-1}. [c] Computed in the gas phase. [d] Computed in a dielectric solvent (ε = 78.4) with the Onsager model and refined with COSMO. [e] Transfer barriers (TB). [f] Endothermicity (E) for principle proton transfer. [g] No distinct barrier.

energetics by the presence of a high dielectric medium (ε = 78.4) where determined by optimizing the reactants, transition states, and products initially with the Onsager model[62] and then subsequently with a single point calculation using COSMO.[74] The energetics are reported in the final columns of Table 4 and reveal a decrease in the barrier for the relaxed proton transfer of from about 1.6–2.2 kcal mol^{-1}. The endothermicities also follow a similar trend in the magnitude of the decrease with the exception of the CF_3-PAA where the solvent makes the reaction to be nearly isoenergetic (+1.15 kcal mol^{-1}). This latter result is not surprising in view of the contact ion pair products which are clearly substantially stabilized in the solvent.

4. Conclusions

Our investigation of various functionalized phosphonic acid molecules reveals that the relatively weak acidity of the phosphonic acid may be enhanced by fluorinating segments in direct proximity to the $-PO_3H$.[27] The present study focuses on a comparison of methyl-, phenyl-, benzyl-, trifluoromethyl- and phenyldifluoromethyl-phosphonic acids. Fully optimized structures of each of the acids with a single water molecule indicate that the water molecule binds more tightly to the fluorinated molecules with corresponding slightly shorter hydrogen bonds (O$\cdots$O $\sim$ 0.03–0.04 Å shorter) than the non-fluorinated molecules. The substituents seemingly have little influence on the conformational (*trans* or *cis*) preference for the acid dimers.

The proton transfer between anhydrides and water molecules is important due to the existence of the condensation reactions in pure phosphonic acid. Similar to the comparisons performed with the monomers, optimized geometries and water binding energies of the anhydrides were determined and a comparison confirms the result that fluorination enhances the binding of water. In contrast to the dimer, the acid–acid proton transfer in the anhydrides seems to be attenuated so much that the restriction on the O–H bond does not have noticeable effects on either the geometries or energetics. Removal of any constraints in the systems typically shifts the position of the transition state towards the products and lowers the proton transfer barrier by as much as 2 kcal mol^{-1}. When no constraints are imposed on the system, proton transfer from the anhydride to a water molecule (primary) is accompanied by a secondary proton transfer (from protonated water molecule back to the anhydride) in all cases except with the trifluoromethyl anhydride where charge separation and formation of a hydronium ion occurs. The coexistent proton transfer associated with the principle transfer provides some insight into the proton transfer behaviour in fluorinated and non-fluorinated systems. It appears that the secondary proton transfer would substantially determine the emergence of transition states and the correlated endothermicities. The enhanced acidity arising from the fluorinated segments seems to postpone the occurrence of accompanying proton transfer and eventually leads to an energy profile that exhibits no barrier and the formation of a contact ion pair involving an hydronium ion. The barriers and endothermicities are significantly reduced if the proton transfers are computed in a high dielectric constant medium with the endothermicity for CF_3-PAA all but disappearing.

Acknowledgements

Support for this work was provided by the Alabama Space Grant Consortium of the Alabama NASA EPSCoR program. The majority of the calculations were performed on the Alabama Supercomputer Center in Huntsville, AL.

References

1 Y. Shao, G. Yin, Z. Wang and Y. Gao, *J. Power Sources*, 2007, **167**, 235–242.
2 K. D. Kreuer, S. J. Paddison, E. Spohr and M. Schuster, *Chem. Rev.*, 2004, **104**, 4637–4678.
3 A. Vishnyakov and A. V. Neimark, *J. Phys. Chem. B*, 2000, **104**, 4471–4478.
4 J. A. Elliott, S. Hanna, A. M. S. Elliott and G. E. Cooley, *Polymer*, 2001, **42**, 2251–2253.
5 P. Commer, A. G. Cherstvy and E. S. A. A. Kornyshev, *Fuel Cells*, 2002, **2**, 127–136.
6 S. S. Jang, V. Molinero, T. Cagin and W. A. Goddard, *J. Phys. Chem. B*, 2004, **108**, 3149–3157.
7 D. Marx, *ChemPhysChem*, 2006, **7**, 1848–1870.
8 N. Agmon, *Chem. Phys. Lett.*, 1995, **244**, 456–462.
9 M. Tuckerman, K. Laasonen, M. Sprik and M. Parrinello, *J. Chem. Phys.*, 1995, **103**, 150.
10 T. J. F. Day, U. W. Schmitt and G. A. Voth, *J. Am. Chem. Soc.*, 2000, **122**, 12027–12028.
11 K. D. Kreuer, *Solid State Ionics*, 1997, **97**, 1–15.
12 K. D. Kreuer, *Solid State Ionics*, 2000, **136–137**, 149–160.
13 T. A. Zawodzinski, C. Derouin, S. Radzinski, R. J. Sherman, V. T. Smith, T. E. Springer and S. Gottesfeld, *J. Electrochem. Soc.*, 1993, **140**, 1041–1047.
14 P. L. Antonucci, A. S. Arico, P. Creti, E. Ramunni and V. Antonucci, *Solid State Ionics*, 1999, **125**, 431–437.
15 S. M. Haile, D. A. Boysen, C. R. I. Chisolm and R. B. Merle, *Nature*, 2001, **410**, 910–912.
16 C. Yang, S. Srinivasan, A. B. Bocarsly, S. Tulyani and J. B. Benziger, *J. Membr. Sci.*, 2004, **237**, 145–161.
17 C. Yang, P. Costamagna, S. Srinivasan, J. Benziger and A. B. Bocarsly, *J. Power Sources*, 2001, **103**, 1–9.
18 Q. Li, R. He, J. O. Jensen and N. J. Bjerrum, *Chem. Mater.*, 2003, **15**, 4896–4915.
19 M. F. H. Schuster and W. H. Meyer, *Annu. Rev. Mater. Res.*, 2003, **33**, 233–261.
20 A. Bozkurt, M. Ise, K. D. Kreuer, W. H. Meyer and G. Wegner, *Solid State Ionics*, 1999, **125**, 225–233.
21 K. D. Kreuer, A. Fuchs, M. Ise, M. Spaeth and J. Maier, *Electrochim. Acta*, 1998, **43**, 1281–1288.
22 M. Schuster, W. H. Meyer, G. Wegner, H. G. Herz, M. Ise, M. Schuster, K. D. Kreuer and J. Maier, *Solid State Ionics*, 2001, **145**, 85–92.
23 H. G. Herz, K. D. Kreuer, J. Maier, G. Scharfenberger, M. F. H. Schuster and W. H. Meyer, *Electrochim. Acta*, 2003, **48**, 2165–2171.
24 T. Sata, T. Yoshida and K. Matsusaki, *J. Membr. Sci.*, 1996, **120**, 101–110.
25 M. Schuster, T. Rager, A. Noda, K. D. Kreuer and J. Maier, *Fuel Cells*, 2005, **5**, 355–365.
26 M. Schuster, K.-D. Kreuer, H. Steininger and J. Maier, *Solid State Ionics*, 2008, **179**, 523–528.
27 H. Steininger, M. Schuster, K. D. Kreuer, A. Kaltbeitzel, B. Bingöl, W. H. Meyer, S. Schauff, G. Brunklaus, J. Maier and H. W. Spiess, *Phys. Chem. Chem. Phys.*, 2007, **9**, 1764–1773.
28 H. Steininger, M. Schuster, K. D. Kreuer and J. Maier, *Solid State Ionics*, 2006, **177**, 2457–2462.
29 S. J. Paddison, K.-D. Kreuer and J. Maier, *Phys. Chem. Chem. Phys.*, 2006, **8**, 4530–4542.
30 L. Yan, S. Zhu, X. Ji and W. Lu, *J. Phys. Chem. B*, 2007, **111**, 6357–6363.

31 L. Vilciauskas, S. J. Paddison and K.-D. Kreuer, *J. Phys. Chem. A*, 2009, **113**, 9193–9201.
32 J. O. Joswig and G. Seifert, *J. Phys. Chem. B*, 2009, **113**, 8475–8480.
33 S. Roy, T. M. Ataol and F. Müller-Plathe, *J. Phys. Chem. B*, 2008, **112**, 7403–7409.
34 S. V. Kotov, S. D. Pedersen, W. Qiu, Z.-M. Qiu and D. J. Burton, *J. Fluorine Chem.*, 1997, **82**, 13–19.
35 S. D. Pedersen, W. Qiu, Z. M. Qiu, S. V. Kotov and D. J. Burton, *J. Org. Chem.*, 1996, **61**, 8024–8031.
36 R. Souzy and B. Ameduri, *Prog. Polym. Sci.*, 2005, **30**, 644–687.
37 C. Stone, T. S. Daynard, L.-Q. Hu, C. Mah and A. E. Steck, *J. New Mater. Electrochem. Sys.*, 2000, **3**, 43.
38 K. Jakoby, K. V. Peinemann and S. P. Nunes, *Macromol. Chem. Phys.*, 2003, **204**, 61–67.
39 E. Parcero, R. Herrera and S. P. Nunes, *J. Membr. Sci.*, 2006, **285**, 206–213.
40 H. R. Allcock, M. A. Hofmann, C. M. Ambler, S. N. Lvov, X. Y. Zhou, E. Chalkova and J. Weston, *J. Membr. Sci.*, 2002, **201**, 47–54.
41 H. R. Allcock and R. M. Wood, *J. Polym. Sci., Part B: Polym. Phys.*, 2006, **44**, 2358–2368.
42 T. Bock, H. Mohwald and R. Mulhaupt, *Macromol. Chem. Phys.*, 2007, **208**, 1324–1340.
43 A. Kaltbeitzel, S. Schauff, H. Steininger, B. Bingöl, G. Brunklaus, W. H. Meyer and H. W. Spiess, *Solid State Ionics*, 2007, **178**, 469–474.
44 Y. J. Lee, B. Bingol, T. Murakhtina, D. Sebastiani, W. H. Meyer, G. Wegner and H. W. Spiess, *J. Phys. Chem. B*, 2007, **111**, 9711–9721.
45 Y. J. Lee, T. Murakhtina, D. Sebastiani and H. W. Spiess, *J. Am. Chem. Soc.*, 2007, **129**, 12406–12407.
46 M. J. Frisch, G. W. Trucks, H. B. Schlegel, G. E. Scuseria, M. A. Robb, J. R. Cheeseman, J. A. Montgomery, Jr., T. Vreven, K. N. Kudin, J. C. Burant, J. M. Millam, S. S. Iyengar, J. Tomasi, V. Barone, B. Mennucci, M. Cossi, G. Scalmani, N. Rega, G. A. Petersson, H. Nakatsuji, M. Hada, M. Ehara, K. Toyota, R. Fukuda, J. Hasegawa, M. Ishida, T. Nakajima, Y. Honda, O. Kitao, H. Nakai, M. Klene, X. Li, J. E. Knox, H. P. Hratchian, J. B. Cross, V. Bakken, C. Adamo, J. Jaramillo, R. Gomperts, R. E. Stratmann, O. Yazyev, A. J. Austin, R. Cammi, C. Pomelli, J. Ochterski, P. Y. Ayala, K. Morokuma, G. A. Voth, P. Salvador, J. J. Dannenberg, V. G. Zakrzewski, S. Dapprich, A. D. Daniels, M. C. Strain, O. Farkas, D. K. Malick, A. D. Rabuck, K. Raghavachari, J. B. Foresman, J. V. Ortiz, Q. Cui, A. G. Baboul, S. Clifford, J. Cioslowski, B. B. Stefanov, G. Liu, A. Liashenko, P. Piskorz, I. Komaromi, R. L. Martin, D. J. Fox, T. Keith, M. A. Al-Laham, C. Y. Peng, A. Nanayakkara, M. Challacombe, P. M. W. Gill, B. G. Johnson, W. Chen, M. W. Wong, C. Gonzalez and J. A. Pople, *GAUSSIAN 03 (Revision C.2)*, Gaussian, Inc., Wallingford, CT, 2004.
47 H. B. Schlegel, *J. Comput. Chem.*, 1982, **3**, 214–218.
48 C. C. J. Roothan, *Rev. Mod. Phys.*, 1951, **23**, 69.
49 J. A. Pople and R. K. Nesbet, *J. Chem. Phys.*, 1954, **22**, 571.
50 R. McWeeny and G. Dierksen, *J. Chem. Phys.*, 1968, **49**, 4852.
51 A. D. Becke, *J. Chem. Phys.*, 1993, **98**, 5648.
52 C. Lee, W. Yang and R. G. Parr, *Phys. Rev. B: Condens. Matter*, 1988, **37**, 785.
53 A. D. McLean and G. S. Chandler, *J. Chem. Phys.*, 1980, **72**, 5639.
54 S. F. Boys and F. Bernardi, *Mol. Phys.*, 1970, **19**, 553–566.
55 S. Simon, M. Duran and J. J. Dannenberg, *J. Chem. Phys.*, 1996, **105**, 11024.
56 N. Kobko and J. J. Dannenberg, *J. Phys. Chem. A*, 2001, **105**, 1944–1950.
57 D. Tzeli, A. Mavridis and S. S. Xantheas, *Chem. Phys. Lett.*, 2001, **340**, 538–546.
58 J. Garza, J. Z. Ramirez and R. Vargas, *J. Phys. Chem. A*, 2005, **109**, 643–651.
59 M. Elstner, P. Hobza, T. Frauenheim, S. Suhai and E. Kaxiras, *J. Chem. Phys.*, 2001, **114**, 5149–5155.
60 S. J. Paddison, *J. New Mater. Electrochem. Sys.*, 2001, **4**, 197–207.
61 J. A. Elliott and S. J. Paddison, *Phys. Chem. Chem. Phys.*, 2007, **9**, 2602–2618.
62 L. Onsager, *J. Am. Chem. Soc.*, 1936, **58**, 1486–1493.
63 M. W. Wong, M. J. Frisch and K. B. Wiberg, *J. Am. Chem. Soc.*, 1991, **113**, 4776–4782.
64 M. W. Wong, K. B. Wiberg and M. J. Frisch, *J. Am. Chem. Soc.*, 1992, **114**, 523–529.
65 M. W. Wong, K. B. Wiberg and M. J. Frisch, *J. Am. Chem. Soc.*, 1992, **114**, 1645–1652.
66 S. J. Paddison, D. W. Reagor and T. A. Zawodzinski Jr, *J. Electroanal. Chem.*, 1998, **459**, 91–97.
67 S. J. Paddison, G. Bender, K. D. Kreuer, N. Nicoloso and T. A. Zawodzinski, *J. New Mater. Electrochem. Sys.*, 2000, **3**, 291–300.
68 R. Paul and S. J. Paddison, *J. Phys. Chem. B*, 2004, **108**, 13231–13241.
69 Z. J. Lu, M. Lanagan, E. Manias and D. D. Macdonald, *J. Phys. Chem. B*, 2009, **113**, 13551–13559.
70 D. Q. Wei and D. R. Salahub, *J. Chem. Phys.*, 1994, **101**, 7633–7642.
71 J. Lobaugh and G. A. Voth, *J. Chem. Phys.*, 1996, **104**, 2056–2069.
72 D. E. Sagnella and M. E. Tuckerman, *J. Chem. Phys.*, 1998, **108**, 2073–2083.
73 S. J. Paddison, *Annu. Rev. Mater. Res.*, 2003, **33**, 289–319.
74 F. Eckert and A. Klamt, *AIChE J.*, 2002, **48**, 369–385.